Resting-State Functional Connectivity Predicts Individual Pain Ratings to a Tonic Orofacial Pain Stimulus

Lizbeth J. Ayoub[1,2,3], Mary Pat McAndrews[2,4], Alexander Barnett[5], Ka Chun Jeremy Ho[1], Iacopo Cioffi[1,3,6], Massieh Moayedi[1,3,6§]

[1] Centre for Multimodal Sensorimotor and Pain Research, Faculty of Dentistry, University of Toronto, Toronto, ON, Canada, M5G 1E2;
[2]Division of Clinical and Computational Neuroscience, Krembil Brain Institute, Toronto Western Hospital, University Health Network, Toronto, ON, Canada, M5T 2S8;
[3]University of Toronto Centre for the Study of Pain, Toronto, ON, Canada, M5T 1P8;
[4]Department of Psychology, University of Toronto, Toronto, ON, Canada;
[5]Center for Neuroscience, University of California at Davis, Davis, California, USA;
[6]Department of Dentistry, Mount Sinai Hospital, Toronto, ON, Canada, M5G 1X5.

Abbreviated title: Baseline neural correlates of an ecologically valid model of orofacial pain

§Please address all correspondence to:
Massieh Moayedi, PhD
Centre for Multimodal Sensorimotor and Pain Research
Faculty of Dentistry, University of Toronto
123 Edward Street, Room 501B
Toronto, ON
Canada M5G 1E2
Email: m.moayedi@utoronto.ca

ABSTRACT

Pain is a subjective experience with significant individual differences. Laboratory studies investigating pain thresholds and acute pain have identified structural and functional neural correlates. However, these types of pain stimuli have limited ecological validity to real-life pain experience. Here, we use an orthodontic procedure which typically induces pain lasting several days. We aimed to determine whether the baseline structure and resting-state functional connectivity (rsFC) of key regions along the trigeminal nociceptive and pain modulatory pathways correlate with subsequent peak pain ratings. Twenty-six healthy individuals underwent structural (T1, diffusion-weighted MRI) and resting-state functional (rs-fMRI) scanning prior to the orthodontic procedure, the insertion of an elastomeric separator between teeth, for five days. Participants recorded pain ratings three times, daily. Peak pain was not correlated with structural measures for the trigeminal nerve or any brain region. However, peak pain correlated with rsFC between the contralateral thalamus and bilateral insula, and negatively correlated with connectivity between the periaqueductal gray and core nodes of the default mode network (medial prefrontal and posterior cingulate cortices). In this ecologically valid model, we demonstrate that both ascending nociceptive and descending pain modulatory pathways shape the individual pain experience.

KEYWORDS: orthodontics, neuroimaging, voxel-based morphometry, diffusion-weighted imaging, individual differences.

INTRODUCTION

Pain perception can vary dramatically between individuals: what feels like a light noxious stimulus to one person may feel excruciating to someone else. This experience is shaped by various factors including biological (e.g. genetics), psychological (e.g. anxiety, catastrophizing) and sociocultural factors (e.g. socioeconomic status) (Coghill et al. 2003; Rollman et al. 2004; Poleshuck and Green 2008; Ong et al. 2010; Cioffi et al. 2016; Lautenbacher et al. 2017; Sorge and Totsch 2017). Greater insight into these individual differences has been provided by brain imaging studies using structural and functional magnetic resonance imaging (sMRI, fMRI) (Coghill et al. 2003; Moulton et al. 2006; Erpelding et al. 2012; Moayedi et al. 2012; Hemington et al. 2017; Hung et al. 2017; Moayedi and Hodaie 2019). Notably, resting-state functional connectivity (rsFC) has been shown to be related to individual differences in pain sensitivity in laboratory-based studies (Cheng et al. 2015; Spisak et al. 2020). However, laboratory-based studies of experimental pain are limited in their ecological validity in evaluating a realistic painful experience. There has been recent interest in identifying brain-based predictors of pain. However, these have relied on multivariate machine learning approaches, which provide limited insight into neural mechanisms (Wager et al. 2013; Woo et al. 2017; Spisak et al. 2020). Here, we investigate whether baseline brain structure and function can predict pain induced by an ecologically valid and clinically relevant tonic orofacial pain stimulus—elastomeric separator insertion.

Orthodontic treatments cause pain in 72-95% of individuals (Kavaliauskiene et al. 2012; Asiry et al. 2014). The placement of an elastomeric separator between molars is an orthodontic procedure that creates space between teeth before brace bonding (Proffit et al. 2019). Orofacial pain induced by the separators in healthy adolescents and adults peaks within 48 hours after insertion, then resolves within 5-7 days (Bergius et al. 2002; Aldrees 2015; Cioffi et al. 2016). The separator compresses the periodontal ligament of the alveolar bone, which induces pressure, inflammation and pain (Krishnan 2007). Pain induced by the separator is shaped by cognitive factors such as somatosensory amplification and trait anxiety (Cioffi et al. 2016).

Pain in the orofacial region is mediated by the trigeminal nociceptive system. The trigeminal nerve carries orofacial nociceptive signals to the brainstem (Sessle 1999), and further to the thalamus and cortex for processing (Davis and Moayedi 2013). The thalamus is a site of nociceptive relay (Coghill et al. 1999; Vogt 2005; Apkarian 2013) and one of the most consistently activated brain regions in response to an orofacial noxious stimulus (Ayoub et al. 2018). The experience of pain is modulated by descending circuits. Notably, the periaqueductal grey (PAG), an opiate-rich region, is a key node of these descending circuits (Millan 2002).

Here, we aim to determine whether key structures of the ascending trigeminal nociceptive system and descending pain modulatory pathways correlate with peak pain intensity induced by an orthodontic separator placement. We hypothesize that pre-existing structure and functional connectivity of regions involved in the trigeminal nociceptive system will predict an individual's pain severity to this ecologically valid pain model. Specifically, we expect that the structural integrity of the trigeminal nerve and grey matter volume of nociceptive processing and pain modulatory brain regions at baseline will correlate with peak pain intensity. We further expect that stronger baseline thalamic and weaker PAG functional connectivity with pain-related brain regions will correlate with peak pain intensity. Finally, we expect that the combined baseline neural correlates of peak pain will better explain individual differences in pain ratings than any measure alone.

MATERIALS AND METHODS

Participants

Twenty-six healthy individuals (11 women, 15 men; 25.7 ± 4.4 years) consented for this study. We obtained approval from University of Toronto Human Research Ethics Board (#32797). We excluded participants based on the following criteria: current pain, history of chronic pain, chronic illness, psychiatric disorder, pregnancy, metal implants, fixed orthodontic retainers, porcelain-fused-to-metal or full metal crowns, severe dental malocclusions, spaces in dental quadrant 4 (lower right mandible;

absence of interproximal tooth contacts), undergoing current orthodontic treatment, use of habitual analgesic medication, and presence of dentures. A clinical examination was performed to ensure they did not have temporomandibular disorders (TMD) using the diagnostic criteria (DC/TMD) (Schiffman et al. 2014). Participants were financially compensated for their time.

Pain Model

An elastomeric separator (American Orthodontics, X-Ring Separators, Sheboygan, USA) was placed at the mesial interproximal contact of the right permanent mandibular first molar by a licensed orthodontist (IC). The separator was kept in place for five days, as previously done (Cioffi et al. 2016). Participants were instructed not to take any analgesics, such as ibuprofen or acetaminophen to reduce pain.

Questionnaires

Pain Diary

We provided a pain diary to participants to record their pain intensity three times per day (10:00, 16:00, 22:00) on a 100 mm visual analogue scale (VAS) over the course of five days following separator placement, as previously done (Cioffi et al. 2016) . The VAS scale had two anchors: left anchor “no pain” and right anchor “worst pain imaginable” (Price et al. 1983).

State-Trait Anxiety Inventory

Participants completed the State-Trait Anxiety Inventory (STAI) before the insertion of the separator (Spielberger et al. 1970). The STAI-trait anxiety (Y-2) is a twenty-item questionnaire, with the scale for each item ranging from 0 to 4 points. It is a self-report questionnaire designed to evaluate trait levels of anxiety. The STAI-state anxiety (Y-1) was not used.

Somatosensory Amplification Scale (SSAS) questionnaire

Participants completed the Somatosensory Amplification Scale (SSAS) questionnaire before the insertion of the separator (Barsky et al. 1988). The SSAS questionnaire is a ten-item questionnaire, scale

for each item ranging from 1 to 5 points. The self-report questionnaire detects whether an individual has a tendency to amplify benign uncomfortable somatic or visceral sensations.

Pain scores analyses

To determine pain scores from the pain diaries, we measured each marking on the pain VAS scale in millimetres and took the average of the three daily pain ratings. As such, each participant had one pain rating per day. The highest average daily pain rating was considered peak pain intensity score for each individual. These scores were used in all neuroimaging analyses.

Daily pain intensity scores (five per individual) were tested for normality using Shapiro-Wilk's test. Given that these were not normally distributed, differences between daily ratings were assessed using Friedman's test, a non-parametric repeated measures ANOVA. Significance was set at $P < 0.05$. Multiple correction of post-hoc tests was performed using Dunn's test. All statistical analyses on pain scores were performed using GraphPad v8.4 (https://graphpad.com).

Relationship between psychological traits and peak pain ratings

Given our previous findings that STAI-trait anxiety and SSAS scores affected the experience of pain induced by elastomeric separators (Cioffi et al. 2016), here, we correlated these psychological measurements with peak pain intensity ratings. We tested the STAI-trait and SSAS scores for normality using Shapiro-Wilk's test. Then, we used Spearman's correlation test to measure the degree of association between each of these scores and peak pain ratings over five days. Significance was set at $P < 0.05$.

Structural and Functional Neuroimaging

All participants underwent magnetic resonance imaging (MRI) before the insertion of the separator. All scans were acquired using a 3T Siemens Prisma-fit MRI scanner equipped with a 32-channel head coil at the Hospital for Sick Children in Toronto, Canada. Participants were asked to "relax and fixate on the crosshair at the center of the display in the scanner, and not to think about anything in particular."

Structural imaging scan

Structural T1-weighted MRI scans were acquired with a magnetization prepared rapid gradient echo (MPRAGE) using the following sequence: echo time (TE) = 2.96ms; repetition time (TR) = 2300ms; inversion time (TI) = 900ms; 256 sagittal slices; flip angle = 9°; in-plane matrix resolution = 256 × 256 and field-of-view = 256 x 256 mm, resulting in a voxel size = 1 x 1 x 1 mm^3; with a GRAPPA acceleration factor = 2.

Functional imaging scan

Rs-fMRI scans were collected using T2*-weighted echo-planar pulse imaging (EPI) sequence, with the following parameters: TE = 30ms, TR = 1500ms, 50 axial slices; flip angle = 70°; in-plane matrix resolution = 74 × 74 and field-of-view = 222 x 222 mm, resulting in a voxel size = 3 x 3 x 3 mm^3; 200 volumes, with a multiband slice acceleration factor = 2, total scan time = 5 minutes.

Diffusion weighted imaging scan

Two sets of diffusion-weighted images were acquired with reverse phase-encode blips (anterior-posterior and posterior-anterior) resulting in images with distortions in opposite directions with the following parameters: 60 non-collinear diffusion encoding directions with b = 1000 s/mm^2, 7 non-diffusion encoding volumes (B0). DWI acquisition used the following sequence: TE = 73ms, TR = 4400ms; 80 slices; flip angle = 90°; in-plane matrix resolution = 122 × 122, field-of-view = 244 x 244 mm, resulting in a 2 mm isotropic voxel size; with a multiband slice acceleration factor = 2.

Neuroimaging analysis

Voxel-Based Morphometry

We sought to determine whether brain grey matter volume correlated with peak pain ratings. To do so, we performed a voxel-based morphometry (VBM) analysis on all anatomical T1 scans (Ashburner and Friston 2000). VBM was performed in SPM v12 (http://www.fil.ion.ucl.ac.uk/spm/software/spm12) running on MATLAB (R2016b v.9.1; Mathworks, Nantick, MA). First, all scans were centered at the anterior commissure, and were segmented into gray matter, white matter and CSF tissues. Next, the DARTEL toolbox was used to iteratively align grey and white matter images to a study specific template aligned to the MNI template space (Ashburner 2007). Images were smoothed using an 8 mm at full-width at half-maximum (FWHM) Gaussian kernel. We performed a voxelwise general linear model to determine whether grey matter volume correlates with peak pain intensity. Significance was set a cluster-corrected $P_{FWE} < 0.05$ (with a cluster-forming height threshold of $P < 0.001$). Total intracranial volume was included in the general linear model as a nuisance covariate.

Diffusion Tensor Imaging

We sought to determine whether microstructure of the cisternal segment of the trigeminal nerve, just outside the pontine trigeminal root-entry zone, is correlated to peak pain ratings. To do so, we performed a diffusion tensor imaging (DTI) analysis using FDT toolbox (FMRIB's Diffusion Toolbox) in FSL 5.0.11 (https://fsl.fmrib.ox.ac.uk/fsl/fslwiki/FDT). Volumes with no diffusion weighting (B0 volumes) underwent topup, which estimates the susceptibility-induced off-resonance field, i.e. distortion in the subject's head (Andersson et al. 2003; Smith et al. 2004). Next, we used the eddy tool to correct for eddy current distortions, susceptibility-induced distortion, and subject movement (Andersson and Sotiropoulos 2016). We then fit a tensor model using DTIFIT on the eddy corrected scans. We identified the cisternal segment of the trigeminal nerve, as previously done (Moayedi et al. 2012; Chen et al. 2016), by overlaying the principal eigenvector (V1) map, colored in RGB, onto and modulated to the FA map for

each subject in FSLeyes (https://git.fmrib.ox.ac.uk/fsl/fsleyes/fsleyes/). Individual masks of the right cisternal segment of the trigeminal nerve were used to extract FA, MD, AD and RD. We tested all DTI metrics for normality using Shapiro-Wilk's test. Then, we tested whether these values were correlated with peak pain ratings using Spearman's correlation. Significance was set at $P < 0.05$.

Seed-to-voxel rsFC analysis

We performed a seed-to-voxel rsFC analysis using CONN v17.f toolbox (http://www.conn-toolbox.org) running on MATLAB (R2016b v.9.1; Mathworks, Nantick, MA). We preprocessed anatomical T1 scans and rs-fMRI scans using tools from the Statistical Parametric Mapping software package (SPM v.12; http://www.fil.ion.ucl.ac.uk/spm/software/spm12) incorporated within CONN. First, we removed five initial scans to allow for field homogeneity. All functional scans underwent realignment, which estimates six parameters of motion and corrects it in the x, y and z planes as well as their rotations, roll, pitch, yaw. Next, we used the ART toolbox, implemented in CONN, to detect outlier scans based on conservative settings (global signal threshold at Z=3; subject motion threshold at 0.5 mm) (Power et al. 2012). Following this step, structural and functional scans underwent grey, white and cerebrospinal fluid (CSF) segmentation, and were normalized to the Montreal Neurological Institute (MNI) standard space template. Scans were resliced using default Tissue Probability Maps (structural and functional target resolution at 2 mm). Functional scans were smoothed using an 8-mm FWHM Gaussian kernel. Preprocessed scans underwent denoising, where aCompCor regressed blood-oxygen-level-dependent (BOLD) signal of non-neuronal origin (Behzadi et al. 2007), and five principal components were derived for each tissue type (white matter and CSF). Additionally, the following confounding variables were regressed from the model using the indicated number of vectors: white matter (5), CSF (5), motion parameters and their temporal derivatives (12), scrubbing (22) and a regressor to model the first 15 frames and its temporal derivative. This last regressor was added to baseline correct after denoising as normally done in CONN (Whitfield-Gabrieli and Nieto-Castanon 2012). To identify low-frequency

fluctuations characterizing resting state connectivity, we applied a band-pass filter of 0.008-0.09Hz to the data. Then, we performed a whole brain seed-to-voxel rsFC with two seeds: the left thalamus, contralateral to the site of separator placement, and the PAG. The left thalamus region-of-interest (ROI) is from the AAL atlas, included with CONN. Given the absence of a PAG ROI in any standard neuroimaging atlas, we defined the PAG ROI based on a meta-analytic search on Neurosynth (https://neurosynth.org) with the term "pain". We extracted the map of all the brain regions that showed activation and selected the PAG cluster. For the first-level rsFC analysis, we used bivariate correlations to quantify connectivity between each seed to every other voxel in the brain within each subject. At second-level analysis, we evaluated the effect of peak pain intensity, accounting for sex in the model, using a non-parametric cluster-mass $P_{FDR} < 0.05$ (cluster-mass-forming height threshold $P_{uncorrected} < 0.001$, 1000 permutations). Sex was included in the model as evidence suggests sex differences in pain and in brain networks (Linnman, Beucke, et al. 2012; Wang et al. 2014; Galli et al. 2016).

Regression Analysis

We performed a linear regression analysis to determine whether the baseline connectivity results explained overlapping or non-overlapping variance in peak pain using IBM SPSS Statistics for Macintosh v.24 (IBM Corp., Armonk, N.Y., USA). We included a composite measure for the ascending nociceptive system findings (thalamic seed) and the descending modulatory system findings (PAG seed) in the regression analysis. Specifically, composite measures were calculated as the mean of the connectivity values from each seed to each resultant target that were significantly correlated to peak pain. The regression model included peak pain as a dependent variable, with sex, thalamic connectivity composite, and PAG connectivity composite as independent variables. The variance inflation factor (VIF) was calculated to evaluate whether the model was susceptible to collinearity.

RESULTS

Pain Ratings

Participants rated a median peak pain intensity following the placement of the separator at 17.2 [5.08-31.83] [IQR]. Pain ratings were the highest within two days, then declining after the second day (Figure 1, see Figure S1 for individual pain ratings). Pain ratings were significantly different across days (χ^2 = 12.51, P = 0.014). Post-hoc paired t-tests revealed that pain ratings on Day 2 (median [IQR]= 8.5 [1.0-25.50]) were significantly greater than pain ratings on Day 5 (3.3 [1.0-12.42]; Dunn-corrected P = 0.044.

Psychological ratings

Participants rated moderate trait anxiety (38.3 ± 11.37 (mean ± standard deviation (SD)), and mid-level somatosensory amplification score (16.3 ± 5.76) (mean ± SD). Peak pain ratings were not correlated with trait anxiety (r = 0.12, P = 0.55) nor somatosensory amplification scores (r = 0.21, P = 0.31).

Neuroimaging

No structural correlates of peak pain intensity

We found no structural correlates of peak pain intensity in our cohort. Specifically, no brain grey matter region's volume correlated with peak pain intensity. Furthermore, DTI metrics of the right cisternal segment of the trigeminal nerve did not correlate with peak pain intensity (FA: r = 0.004, P = 0.98; MD: r = 0.004, P = 0.98; RD: r = 0.022, P = 0.92; and AD: r = -0.031, P = 0.88).

Stronger thalamo-insular rsFC correlates with peak pain intensity

We found that rsFC between the left thalamus and bilateral insula significantly correlated with peak pain: L Thalamus-Insula (peak MNI coordinates (X,Y,Z) = -38, -8, 0, cluster size: 743 mm^3) at r^2 = 0.62 and L Thalamus-R Insula (peak MNI coordinates (X,Y,Z) = 38, 0, -14, cluster size: 513 mm^3) at r^2 =

0.54, cluster-mass $P_{FDR} < 0.05$ (Figure 2). In other words, participants who had stronger connectivity between these regions rated their peak pain rating as higher.

Weaker PAG-default mode network rsFC correlates with peak pain intensity

We found that PAG rsFC to nodes of default mode network (DMN) significantly correlated negatively with peak pain intensity: the right medial prefrontal cortex (mPFC; peak MNI coordinates (X,Y,Z): 12 44 -12, cluster size : 456 mm^3) at $r^2 = 0.66$ and the left posterior cingulate cortex (PCC; peak MNI coordinates (X,Y,Z): -12 -46 28, cluster size: 254 mm^3) at $r^2 = 0.60$, cluster-mass $P_{FDR} < 0.05$ (Figure 3). In other words, participants who had weaker connectivity between these regions rated their peak pain as higher.

Ascending nociceptive and descending modulatory systems account for non-overlapping variance of peak pain

To determine whether thalamo-insular connectivity and PAG-DMN connectivity explained overlapping or non-overlapping variance in peak pain, we performed a regression analysis with both rsFC measures input into the same model. We included biological sex in the model. The combined model was significantly related to peak pain, adjusted $r^2 = 0.78$, $F_{3,22} = 30.95$, $P < 0.001$. In other words, the model accounted for 78% of the variance in peak pain ratings. The VIF of all predictors was < 2 indicating that the model did not suffer from collinearity (Hair et al. 1995; Menard 1995). Importantly, connectivity findings were independently predictive of peak pain in this joint model (thalamo-insular connectivity, $\beta = 0.42$, $t_{22} = 3.42$, $P = 0.002$; PAG-DMN connectivity, $\beta = -0.54$, $t_{22} = -4.38$, $P < 0.001$) with thalamo-insular connectivity explaining 10% of the unique variance in peak pain and PAG connectivity explaining 17% of the unique variance in peak pain. Biological sex was not a significant predictor in this joint model (Sex [Male=1; Female=0], $\beta = -0.15$, $t_{22} = -1.64$, $P = 0.12$).

DISCUSSION

The pain experience can vary dramatically from person to person. Individual variability in pain is thought to be correlated to the structure and functional connectivity of nociceptive-responsive and pain modulatory regions. Here, we used an ecologically valid model of tonic orofacial pain to evaluate whether baseline trigeminal and grey matter structure, as well as rsFC of brain regions involved in nociceptive processing and pain modulation correlate with peak pain intensity, occurring days later. Pain intensity was highest within 48 hours (Figure 1). Although, we did not find any significant structural correlates of peak pain intensity, we did find significant correlations between peak pain and rsFC of key nodes of both the ascending nociceptive and the descending pain modulatory systems. Specifically, peak pain intensity correlated with stronger rsFC between the thalamus and bilateral insula—a key set of brain region involved in nociceptive processing (Figure 2). Peak pain intensity also correlated with weaker rsFC between the PAG with the mPFC and PCC, core nodes of the DMN (Figure 3). We further showed that together thalamo-insular and PAG-DMN connectivity explained 78% of the variance in pain ratings (in a model that also contained sex), and each explained 10% and 17% of unique variance, respectively, indicating that both ascending and descending systems shape peak pain ratings. Together, these data show that pre-existing rsFC networks may serve as predictors of forthcoming pain intensity to an ecologically valid clinical model of low-level tonic orofacial pain.

Elastomeric separator placement is a common and safe orthodontic procedure. These separators typically induce low to mid-level pain (Bondemark et al. 2004). Overall, our participants had a median of low-level pain compared to previous work in adolescents and adults, who reported moderate levels of pain (Bergius et al. 2002; Bondemark et al. 2004; Aldrees 2015; Cioffi et al. 2016). In contrast, these studies placed more than one separator between the first molar and second premolar, which could explain higher pain intensity ratings compared to our study. Since the amount of pain is proportional to the magnitude of the orthodontic force applied to the teeth (Jones and Chan 1992), increasing the number of separators

can be used in future studies to elucidate the effects of different intensities of tonic nociceptive input. Nevertheless, our findings are consistent with these and other previous studies showing pain intensity is highest within two days of separator placement and resolves by approximately five days after the procedure (Ngan et al. 1989; Bondemark et al. 2004; Kavaliauskiene et al. 2012). Although peak pain intensity in our cohort was variable amongst participants (Figure S1), the temporal pattern was similar to what has been reported, such that Day 2 had a significantly higher median rating than Day 5.

Separator placement is an ecologically valid noxious stimulus as it mimics naturally occurring painful experiences. The model captures environmental variability, such that the individual leaves the laboratory setting, while continuously receiving the stimulus for the duration of the separator placement and as the participant goes through their day. This ecological variability is fundamental to capturing individual differences in pain, particularly in its evolution and resolution. Therefore, this model circumvents the limitations of laboratory-based pain testing, where stimuli are usually brief (i.e., do not go beyond the experimental session), and only capture a brief snapshot of the experience in a controlled setting (Reddy et al. 2012). Critically, this stimulus modality opens a window of opportunity to identify baseline predictors for underlying continuous nociceptive, habituation and antinociceptive mechanisms in the orofacial region.

Functional brain networks are continuously active at rest, including those involved in nociceptive processing and pain modulation (Smith et al. 2009). Previous studies in healthy adults show increased rsFC between brain regions involved in pain processing before administrating nociceptive stimuli, i.e. pain anticipation (Boly et al. 2007; Ploner et al. 2010) and following nociceptive stimulation (Riedl et al. 2011). Analogous to the current findings, a recent study demonstrated that data-driven, multivariate analyses of rsFC in a pain-free state predicted individual differences in pain sensitivity during later testing (Spisak et al., 2020). Their measure of pain sensitivity was a ‘composite’ based on a weighted

average of heat, cold and mechanical pain thresholds delivered 1-3 days from the time of resting-state functional imaging. Notably, pain thresholds measure a brief static point at which the stimulus becomes painful for the individual (Rolke et al. 2006). These do not reflect most real-life painful experiences. In contrast, our study shows that both ascending and descending networks predict individual peak pain induced by an ecologically valid tonic noxious stimulus.

We investigated the rsFC of the thalamus, a major relay region of the ascending nociceptive pathways (Craig et al. 1994). The thalamus and insula are structurally connected. Evidence from primates and humans show efferent and afferent projections from the dorsal thalamus to the insular cortex (Augustine 1996). The dorsal thalamus projects to the insula from the ventral anterior, centromedian, ventral posterior medial (VPM) nuclei (Augustine 1985). Specifically, there is evidence that the ventral medial posterior (VMpo) thalamus projects to posterior insula (Craig et al. 1994; Davis et al. 1999; Craig 2014). There is a functional dichotomy in the involvement of the insula in pain perception: the anterior insula is closely associated with the cognitive and/or modulatory aspect of pain, whereas the posterior and mid-insula are associated with lower-level, sensory-discriminative features of pain, such as location and intensity (Brooks et al. 2005; Moayedi 2014; Wiech et al. 2014). Some have even proposed that the posterior insula/opercular region could serve as primary pain cortex (Garcia-Larrea 2012). Our insular clusters are located in the posterior and mid-insula, and therefore receive direct input from the thalamus, and may reflect the first cortical relays of nociceptive information processing. Therefore, our study advances this finding by showing that baseline thalamo-insular connectivity can predict peak pain intensity, and thus supports the sensory-discriminative role of the insula in pain.

Pain perception is a fine balance between nociceptive and antinociceptive mechanisms (Bingel et al. 2007). Early evidence in rodents (Reynolds 1969) and humans (Hosobuchi et al. 1977) implicate the PAG in pain inhibitory mechanisms. More recent evidence suggests that the PAG is involved in both

facilitatory and inhibitory pain mechanisms (Linnman, Moulton, et al. 2012). Our results show that peak pain intensity was negatively correlated with PAG-DMN rsFC. The mPFC, except the medial orbitofrontal cortex, projects directly to the PAG (Leonard 1969; Hardy and Leichnetz 1981, 1981). The PAG receives cortical input as well as input from ascending systems, and projects to brainstem pain modulatory circuits, and is a source of opioidergic pain modulation (Hardy and Leichnetz 1981; Millan 2002; Linnman, Moulton, et al. 2012). Specifically, the dorsolateral and lateral subregions of the PAG receive input from the mPFC and PCC (Linnman, Moulton, et al. 2012). The mPFC, PCC and lateral parietal cortices are regions whose activity is highly correlated and form the DMN (Raichle 2015). DMN activity increases when the individual is not attending to external stimuli and is involved in monitoring the internal milieu which would include monitoring nociceptive signals. We found that individuals who felt less pain had a stronger baseline PAG-DMN rsFC. Previous evidence shows that stronger PAG-DMN rsFC is associated with the tendency to disengage from pain, in other words mind wander away from pain (Kucyi et al. 2013). Thus, high baseline connectivity between the PAG and DMN may enable greater engagement of descending systems in order to disengage from pain. Conversely, weaker PAG-mPFC rsFC in patients with chronic low back pain was related to higher pain intensity conditions, suggesting dysfunction in the descending pain modulation (Yu et al. 2014). As such, our study further postulates that the strength of PAG-DMN rsFC at baseline in the healthy individuals predicts peak pain intensity days later. Whether this rsFC could predict either the development or maintenance of chronic pain requires further investigation.

We further demonstrate that our rsFC findings have partially overlapping, but unique contributions to peak pain intensity induced by separator placement. Together thalamo-insular and PAG-DMN rsFC in the pain-free state, predict peak pain intensity at 78%, days later. Specifically, our model found medium to large unique contributions of the ascending nociceptive system (10%) and descending pain modulation (17%). However, sex did not show meaningful individual contributions to the variance

observed in our data. Thus, the majority of the explained variance is overlapping between the ascending and descending systems—individuals with higher PAG-DMN connectivity also tended to have lower thalamic-insular connectivity and this connectivity phenotype is associated with lower peak pain. However, as mentioned above, each system still showed a significant unique contribution beyond this shared component. These findings suggest that the pre-existing state of the ascending and descending pathways may lead to pain susceptibility and that both systems are required to better predict a painful response to a nociceptive stimulus.

In conclusion, we have used a common orthodontic procedure, separator placement, to investigate pre-existing structural and functional predictors of pain intensity using neuroimaging for the first time. We propose that rsFC of the thalamus and PAG regions in the pain-free state predict peak pain intensity to an ecologically valid pain model in healthy individuals.

ACKNOWLEDGEMENTS

LA is supported by Canadian Institutes of Health Research (CIHR) Frederick Banting and Charles Best Doctoral Research Award. AB is supported by an NSERC Postdoctoral Fellowship Award. KCJH was supported by a CIHR summer studentship award. MM acknowledges support from the Bertha Rosenstadt Endowment Fund. He also holds a National Science and Engineering Research Council Discovery Grant RGPIN-2018-04908. The study was funded by the American Association of Orthodontists Foundation through an Orthodontic Faculty Development Fellowship awarded to IC. We would like to thank Ms. Sinéad Devitt for her help with the diffusion imaging analysis.

AUTHORS CONTRIBUTIONS:

LA: data analysis and drafting of manuscript; MPM: revising the manuscript; AB: data analysis; KCJH: data collection; IC and MM: conception and study design, revising the manuscript. All authors have approved the final version and agree to be accountable for all aspects of the work.

CONFLICTS OF INTEREST

No conflicts to report.

REFERENCES

Aldrees AM. 2015. Intensity of pain due to separators in adolescent orthodontic patients. J Orthod Sci. 4:118-122.

Andersson JL, Skare S, Ashburner J. 2003. How to correct susceptibility distortions in spin-echo echo-planar images: application to diffusion tensor imaging. Neuroimage. 20:870-888.

Andersson JLR, Sotiropoulos SN. 2016. An integrated approach to correction for off-resonance effects and subject movement in diffusion MR imaging. Neuroimage. 125:1063-1078.

Apkarian AV. 2013. A brain signature for acute pain. Trends Cogn Sci. 17:309-310.

Ashburner J. 2007. A fast diffeomorphic image registration algorithm. Neuroimage. 38:95-113.

Ashburner J, Friston KJ. 2000. Voxel-based morphometry--the methods. Neuroimage. 11:805-821.

Asiry MA, Albarakati SF, Al-Marwan MS, Al-Shammari RR. 2014. Perception of pain and discomfort from elastomeric separators in Saudi adolescents. Saudi Med J. 35:504-507.

Augustine JR. 1985. The insular lobe in primates including humans. Neurol Res. 7:2-10.

Augustine JR. 1996. Circuitry and functional aspects of the insular lobe in primates including humans. Brain Res Brain Res Rev. 22:229-244.

Ayoub LJ, Seminowicz DA, Moayedi M. 2018. A meta-analytic study of experimental and chronic orofacial pain excluding headache disorders. Neuroimage Clin. 20:901-912.

Barsky AJ, Goodson JD, Lane RS, Cleary PD. 1988. The amplification of somatic symptoms. Psychosom Med. 50:510-519.

Behzadi Y, Restom K, Liau J, Liu TT. 2007. A component based noise correction method (CompCor) for BOLD and perfusion based fMRI. Neuroimage. 37:90-101.

Bergius M, Berggren U, Kiliaridis S. 2002. Experience of pain during an orthodontic procedure. Eur J Oral Sci. 110:92-98.

Bingel U, Schoell E, Herken W, Buchel C, May A. 2007. Habituation to painful stimulation involves the antinociceptive system. Pain. 131:21-30.

Boly M, Balteau E, Schnakers C, Degueldre C, Moonen G, Luxen A, Phillips C, Peigneux P, Maquet P, Laureys S. 2007. Baseline brain activity fluctuations predict somatosensory perception in humans. Proc Natl Acad Sci U S A. 104:12187-12192.

Bondemark L, Fredriksson K, Ilros S. 2004. Separation effect and perception of pain and discomfort from two types of orthodontic separators. World J Orthod. 5:172-176.

Brooks JC, Zambreanu L, Godinez A, Craig AD, Tracey I. 2005. Somatotopic organisation of the human insula to painful heat studied with high resolution functional imaging. Neuroimage. 27:201-209.

Chen DQ, DeSouza DD, Hayes DJ, Davis KD, O'Connor P, Hodaie M. 2016. Diffusivity signatures characterize trigeminal neuralgia associated with multiple sclerosis. Mult Scler. 22:51-63.

Cheng JC, Erpelding N, Kucyi A, DeSouza DD, Davis KD. 2015. Individual Differences in Temporal Summation of Pain Reflect Pronociceptive and Antinociceptive Brain Structure and Function. J Neurosci. 35:9689-9700.

Cioffi I, Michelotti A, Perrotta S, Chiodini P, Ohrbach R. 2016. Effect of somatosensory amplification and trait anxiety on experimentally induced orthodontic pain. Eur J Oral Sci. 124:127-134.

Coghill RC, McHaffie JG, Yen YF. 2003. Neural correlates of interindividual differences in the subjective experience of pain. Proc Natl Acad Sci U S A. 100:8538-8542.

Coghill RC, Sang CN, Maisog JM, Iadarola MJ. 1999. Pain intensity processing within the human brain: a bilateral, distributed mechanism. J Neurophysiol. 82:1934-1943.

Craig AD. 2014. Topographically organized projection to posterior insular cortex from the posterior portion of the ventral medial nucleus in the long-tailed macaque monkey. J Comp Neurol. 522:36-63.

Craig AD, Bushnell MC, Zhang ET, Blomqvist A. 1994. A thalamic nucleus specific for pain and temperature sensation. Nature. 372:770-773.

Davis KD, Lozano RM, Manduch M, Tasker RR, Kiss ZH, Dostrovsky JO. 1999. Thalamic relay site for cold perception in humans. J Neurophysiol. 81:1970-1973.

Davis KD, Moayedi M. 2013. Central mechanisms of pain revealed through functional and structural MRI. J Neuroimmune Pharmacol. 8:518-534.

Erpelding N, Moayedi M, Davis KD. 2012. Cortical thickness correlates of pain and temperature sensitivity. Pain. 153:1602-1609.

Galli G, Santarnecchi E, Feurra M, Bonifazi M, Rossi S, Paulus MP, Rossi A. 2016. Individual and sex-related differences in pain and relief responsiveness are associated with differences in resting-state functional networks in healthy volunteers. Eur J Neurosci. 43:486-493.

Garcia-Larrea L. 2012. The posterior insular-opercular region and the search of a primary cortex for pain. Neurophysiol Clin. 42:299-313.

Hair JF, Jr. A, R. E., , Tatham RL, Black WC. 1995. Multi-variate data analysis New York, NY: Macmillan.

Hardy SG, Leichnetz GR. 1981. Cortical projections to the periaqueductal gray in the monkey: a retrograde and orthograde horseradish peroxidase study. Neurosci Lett. 22:97-101.

Hardy SG, Leichnetz GR. 1981. Frontal cortical projections to the periaqueductal gray in the rat: a retrograde and orthograde horseradish peroxidase study. Neurosci Lett. 23:13-17.

Hemington KS, Cheng JC, Bosma RL, Rogachov A, Kim JA, Davis KD. 2017. Beyond Negative Pain-Related Psychological Factors: Resilience Is Related to Lower Pain Affect in Healthy Adults. J Pain. 18:1117-1128.

Hosobuchi Y, Adams JE, Linchitz R. 1977. Pain relief by electrical stimulation of the central gray matter in humans and its reversal by naloxone. Science. 197:183-186.

Hung PS, Chen DQ, Davis KD, Zhong J, Hodaie M. 2017. Predicting pain relief: Use of pre-surgical trigeminal nerve diffusion metrics in trigeminal neuralgia. Neuroimage Clin. 15:710-718.

Jones M, Chan C. 1992. The pain and discomfort experienced during orthodontic treatment: a randomized controlled clinical trial of two initial aligning arch wires. Am J Orthod Dentofacial Orthop. 102:373-381.

Kavaliauskiene A, Smailiene D, Buskiene I, Keriene D. 2012. Pain and discomfort perception among patients undergoing orthodontic treatment: results from one month follow-up study. Stomatologija. 14:118-125.

Krishnan V. 2007. Orthodontic pain: from causes to management--a review. Eur J Orthod. 29:170-179.

Kucyi A, Salomons TV, Davis KD. 2013. Mind wandering away from pain dynamically engages antinociceptive and default mode brain networks. Proc Natl Acad Sci U S A. 110:18692-18697.

Lautenbacher S, Peters JH, Heesen M, Scheel J, Kunz M. 2017. Age changes in pain perception: A systematic-review and meta-analysis of age effects on pain and tolerance thresholds. Neurosci Biobehav Rev. 75:104-113.

Leonard CM. 1969. The prefrontal cortex of the rat. I. Cortical projection of the mediodorsal nucleus. II. Efferent connections. Brain Res. 12:321-343.

Linnman C, Beucke JC, Jensen KB, Gollub RL, Kong J. 2012. Sex similarities and differences in pain-related periaqueductal gray connectivity. Pain. 153:444-454.

Linnman C, Moulton EA, Barmettler G, Becerra L, Borsook D. 2012. Neuroimaging of the periaqueductal gray: state of the field. Neuroimage. 60:505-522.

Menard S. 1995. Applied logistic regression analysis: Sage University series on quantitative applications in the social sciences. Thousand Oaks, CA: Sage.

Millan MJ. 2002. Descending control of pain. Prog Neurobiol. 66:355-474.

Moayedi M. 2014. All roads lead to the insula. Pain. 155:1920-1921.

Moayedi M, Hodaie M. 2019. Trigeminal nerve and white matter brain abnormalities in chronic orofacial pain disorders. Pain Rep. 4:e755.

Moayedi M, Weissman-Fogel I, Salomons TV, Crawley AP, Goldberg MB, Freeman BV, Tenenbaum HC, Davis KD. 2012. White matter brain and trigeminal nerve abnormalities in temporomandibular disorder. Pain. 153:1467-1477.

Moulton EA, Keaser ML, Gullapalli RP, Maitra R, Greenspan JD. 2006. Sex differences in the cerebral BOLD signal response to painful heat stimuli. Am J Physiol Regul Integr Comp Physiol. 291:R257-267.

Ngan P, Kess B, Wilson S. 1989. Perception of discomfort by patients undergoing orthodontic treatment. Am J Orthod Dentofacial Orthop. 96:47-53.

Ong AD, Zautra AJ, Reid MC. 2010. Psychological resilience predicts decreases in pain catastrophizing through positive emotions. Psychol Aging. 25:516-523.

Ploner M, Lee MC, Wiech K, Bingel U, Tracey I. 2010. Prestimulus functional connectivity determines pain perception in humans. Proc Natl Acad Sci U S A. 107:355-360.

Poleshuck EL, Green CR. 2008. Socioeconomic disadvantage and pain. Pain. 136:235-238.

Power JD, Barnes KA, Snyder AZ, Schlaggar BL, Petersen SE. 2012. Spurious but systematic correlations in functional connectivity MRI networks arise from subject motion. Neuroimage. 59:2142-2154.

Price DD, McGrath PA, Rafii A, Buckingham B. 1983. The validation of visual analogue scales as ratio scale measures for chronic and experimental pain. Pain. 17:45-56.

Proffit WR, Fields HW, Larson BE, Sarver DM. 2019. Contemporary Orthodontics: Elsevier Health Sciences.

Raichle ME. 2015. The brain's default mode network. Annu Rev Neurosci. 38:433-447.

Reddy KS, Naidu MU, Rani PU, Rao TR. 2012. Human experimental pain models: A review of standardized methods in drug development. J Res Med Sci. 17:587-595.

Reynolds DV. 1969. Surgery in the rat during electrical analgesia induced by focal brain stimulation. Science. 164:444-445.

Riedl V, Valet M, Woller A, Sorg C, Vogel D, Sprenger T, Boecker H, Wohlschlager AM, Tolle TR. 2011. Repeated pain induces adaptations of intrinsic brain activity to reflect past and predict future pain. Neuroimage. 57:206-213.

Rolke R, Magerl W, Campbell KA, Schalber C, Caspari S, Birklein F, Treede RD. 2006. Quantitative sensory testing: a comprehensive protocol for clinical trials. Eur J Pain. 10:77-88.

Rollman GB, Abdel-Shaheed J, Gillespie JM, Jones KS. 2004. Does past pain influence current pain: biological and psychosocial models of sex differences. Eur J Pain. 8:427-433.

Schiffman E, Ohrbach R, Truelove E, Look J, Anderson G, Goulet JP, List T, Svensson P, Gonzalez Y, Lobbezoo F, Michelotti A, Brooks SL, Ceusters W, Drangsholt M, Ettlin D, Gaul C, Goldberg LJ, Haythornthwaite JA, Hollender L, Jensen R, John MT, De Laat A, de Leeuw R, Maixner W, van der Meulen M, Murray GM, Nixdorf DR, Palla S, Petersson A, Pionchon P, Smith B, Visscher CM, Zakrzewska J, Dworkin SF, International Rdc/Tmd Consortium Network IafDR, Orofacial Pain Special Interest Group IAftSoP. 2014. Diagnostic Criteria for Temporomandibular Disorders (DC/TMD) for Clinical and Research Applications: recommendations of the International RDC/TMD Consortium Network* and Orofacial Pain Special Interest Groupdagger. J Oral Facial Pain Headache. 28:6-27.

Sessle BJ. 1999. Neural mechanisms and pathways in craniofacial pain. Can J Neurol Sci. 26 Suppl 3:S7-11.

Smith SM, Fox PT, Miller KL, Glahn DC, Fox PM, Mackay CE, Filippini N, Watkins KE, Toro R, Laird AR, Beckmann CF. 2009. Correspondence of the brain's functional architecture during activation and rest. Proc Natl Acad Sci U S A. 106:13040-13045.

Smith SM, Jenkinson M, Woolrich MW, Beckmann CF, Behrens TE, Johansen-Berg H, Bannister PR, De Luca M, Drobnjak I, Flitney DE, Niazy RK, Saunders J, Vickers J, Zhang Y, De Stefano N, Brady JM, Matthews PM. 2004. Advances in functional and structural MR image analysis and implementation as FSL. Neuroimage. 23 Suppl 1:S208-219.

Sorge RE, Totsch SK. 2017. Sex Differences in Pain. J Neurosci Res. 95:1271-1281.

Spielberger CD, Gorusch RL, Lushene RE. 1970. Manual of the State-Trait Anxiety Inventory.

Spisak T, Kincses B, Schlitt F, Zunhammer M, Schmidt-Wilcke T, Kincses ZT, Bingel U. 2020. Pain-free resting-state functional brain connectivity predicts individual pain sensitivity. Nat Commun. 11:187.

Vogt BA. 2005. Pain and emotion interactions in subregions of the cingulate gyrus. Nat Rev Neurosci. 6:533-544.

Wager TD, Atlas LY, Lindquist MA, Roy M, Woo CW, Kross E. 2013. An fMRI-based neurologic signature of physical pain. N Engl J Med. 368:1388-1397.

Wang G, Erpelding N, Davis KD. 2014. Sex differences in connectivity of the subgenual anterior cingulate cortex. Pain. 155:755-763.

Whitfield-Gabrieli S, Nieto-Castanon A. 2012. Conn: a functional connectivity toolbox for correlated and anticorrelated brain networks. Brain Connect. 2:125-141.

Wiech K, Jbabdi S, Lin CS, Andersson J, Tracey I. 2014. Differential structural and resting state connectivity between insular subdivisions and other pain-related brain regions. Pain. 155:2047-2055.

Woo CW, Schmidt L, Krishnan A, Jepma M, Roy M, Lindquist MA, Atlas LY, Wager TD. 2017. Quantifying cerebral contributions to pain beyond nociception. Nat Commun. 8:14211.

Yu R, Gollub RL, Spaeth R, Napadow V, Wasan A, Kong J. 2014. Disrupted functional connectivity of the periaqueductal gray in chronic low back pain. Neuroimage Clin. 6:100-108.

FIGURES

Figure 1. Pain ratings in response to the orthodontic separator for five days. Self-report median pain ratings (IQR) are represented for all participants (n=26) per day. *Pain ratings on Day 2 were significantly increased than on Day 5, significant at $P < 0.05$. *Abbreviations: IQR* interquartile range *VAS* visual analogue scale.

Figure 2. Increased Thalamo-insular rsFC correlates with peak pain intensity. Resting-state functional connectivity (rsFC) between the left thalamus and bilateral insula before the insertion of the orthodontic separator correlates with peak pain intensity measured on a 100-mm visual analogue scale (VAS), significant at cluster-mass $P_{FDR} < 0.05$.

Figure 3. Decreased PAG-DMN correlates with peak pain intensity. Resting-state functional connectivity (rsFC) of the periaqueductal gray (PAG) and core nodes of the default mode network (DMN)—the posterior cingulate cortex (PCC) and medial prefrontal cortex (mPFC)—before the insertion of the orthodontic separator negatively correlates with peak pain intensity measured on a 100-mm visual analogue scale (VAS), significant at cluster-mass $P_{FDR} < 0.05$.

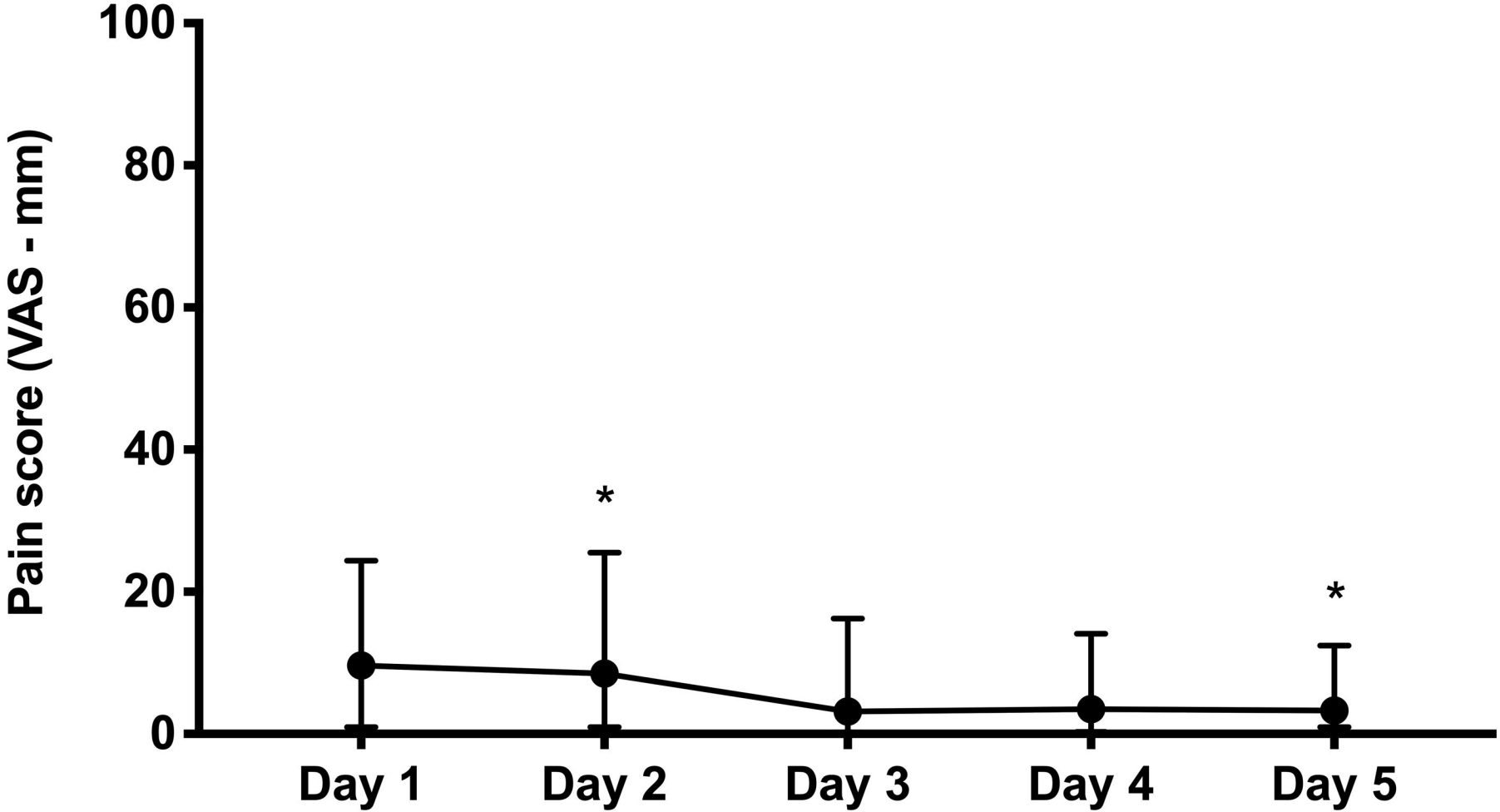
Pain score (VAS - mm)
100
80
60
40
20
0
*
*
Day 1
Day 2
Day 3
Day 4
Day 5

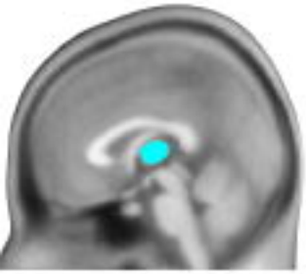

L Thalamus seed

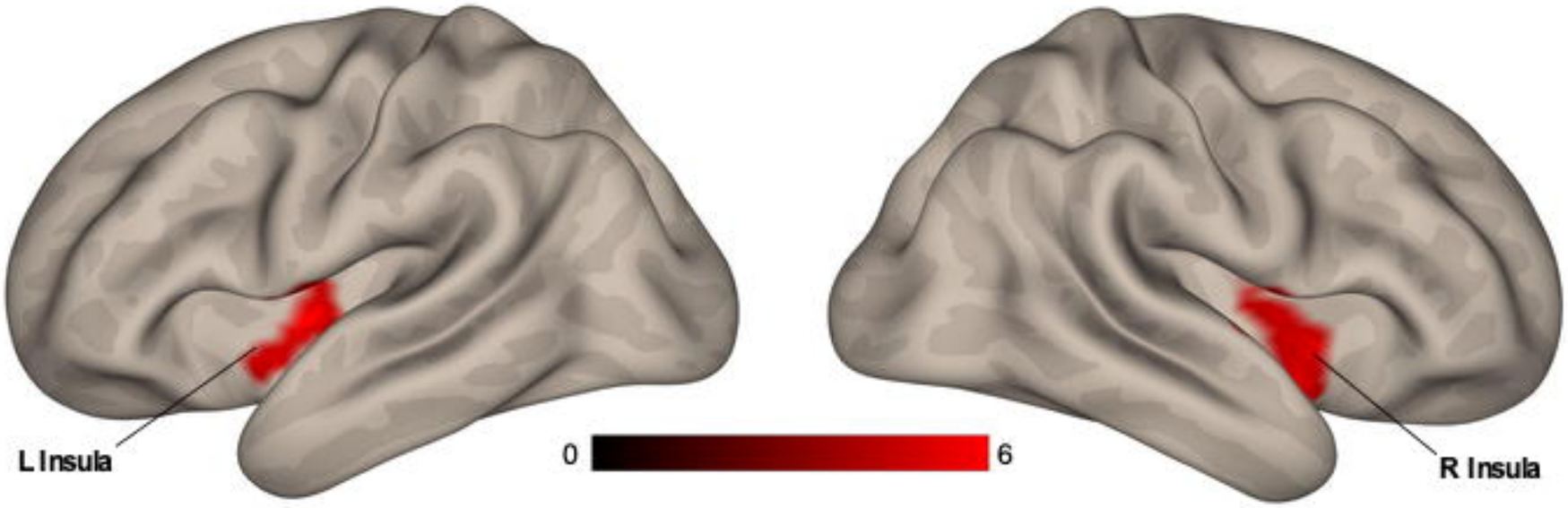

L Thalamus - L Insula

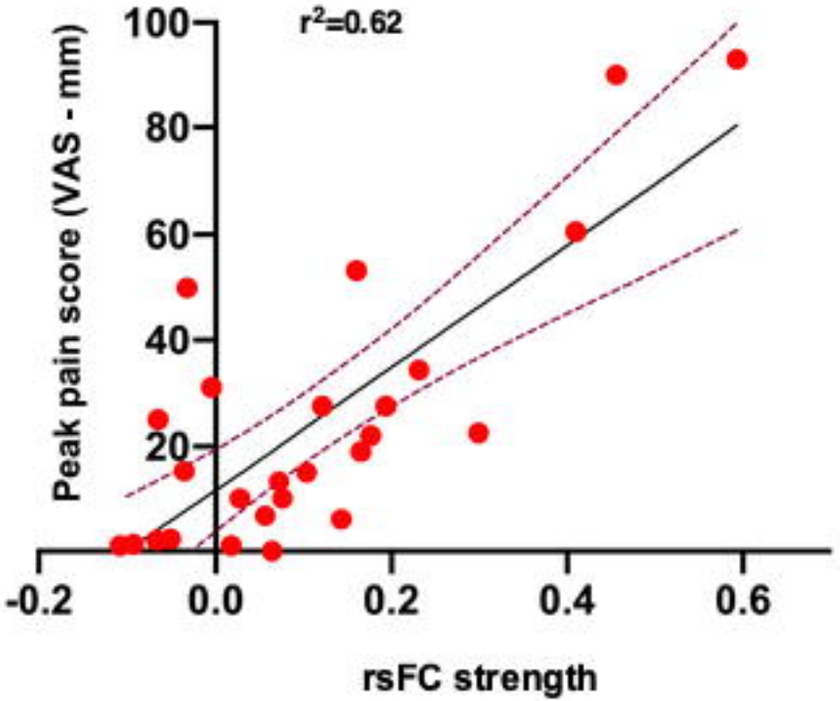

L Thalamus - R Insula

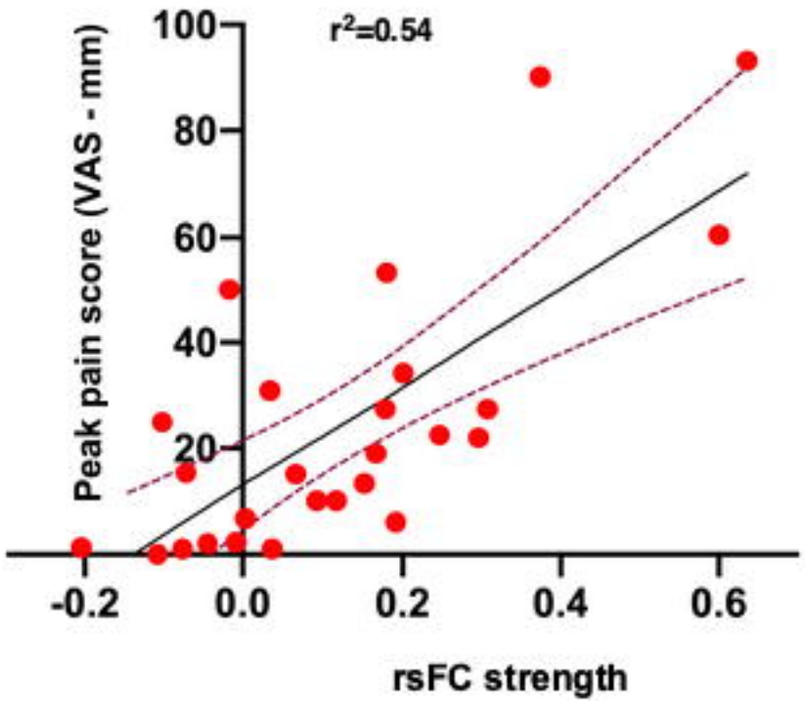

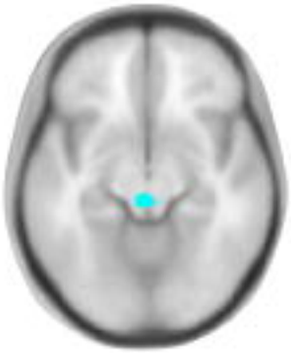

PAG seed

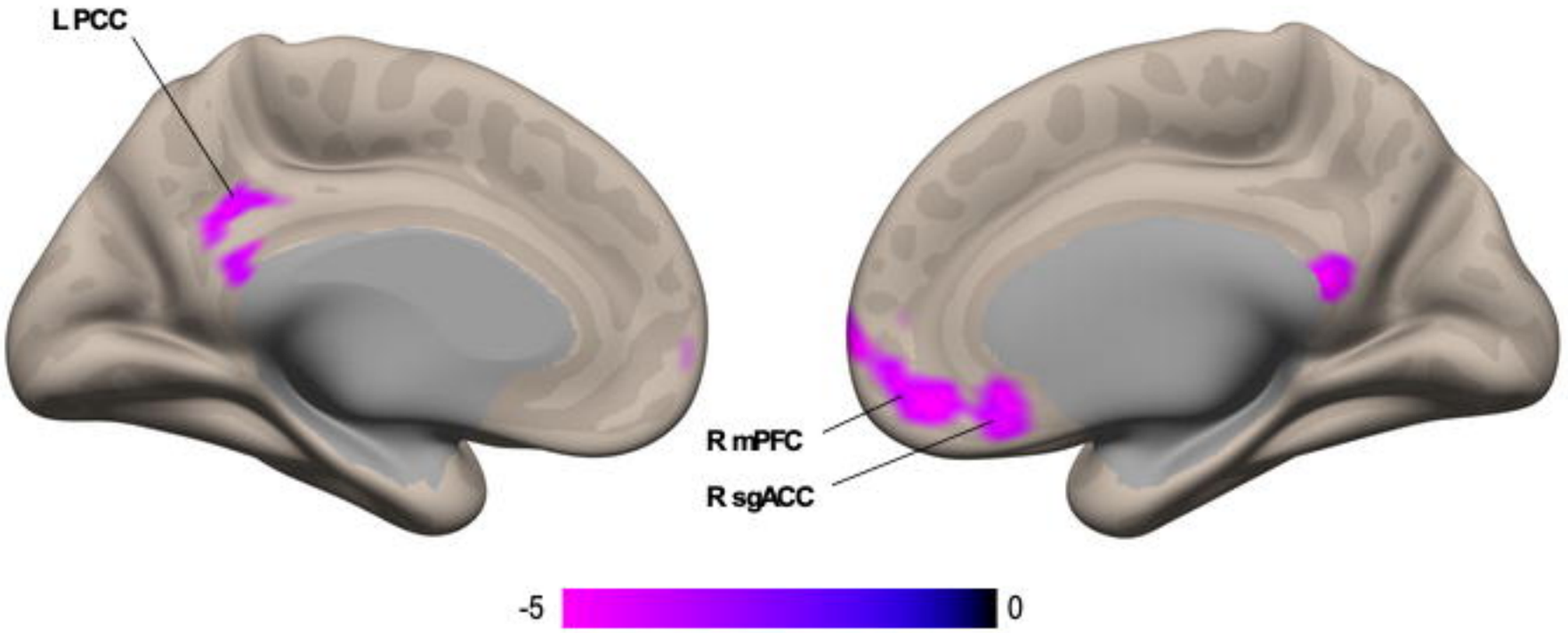
L PCC
R mPFC
R sgACC
-5
0

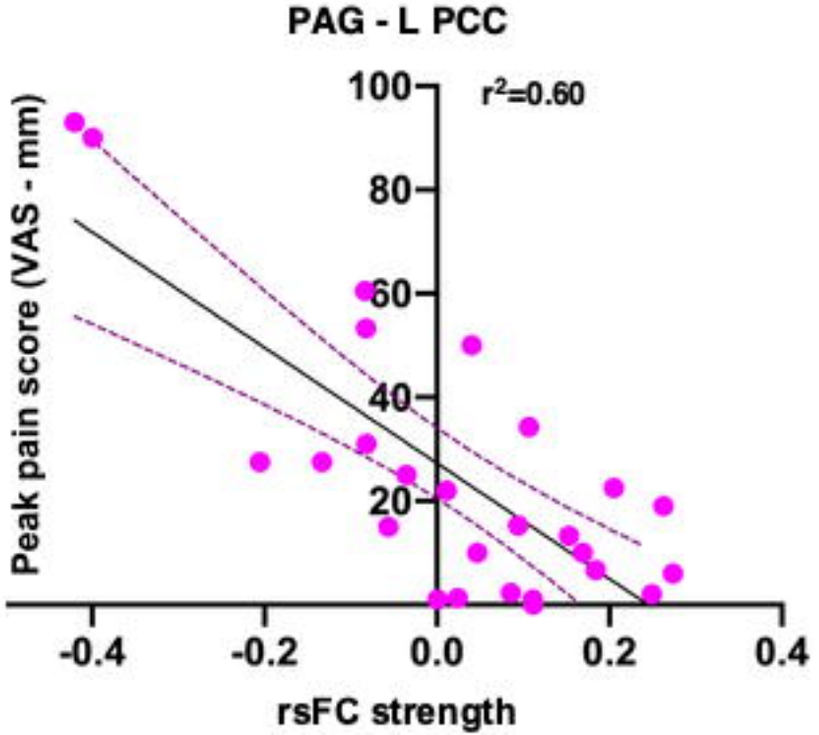
PAG - L PCC
r²=0.60
Peak pain score (VAS - mm)
100
80
60
40
20
-0.4
-0.2
0.0
0.2
0.4
rsFC strength

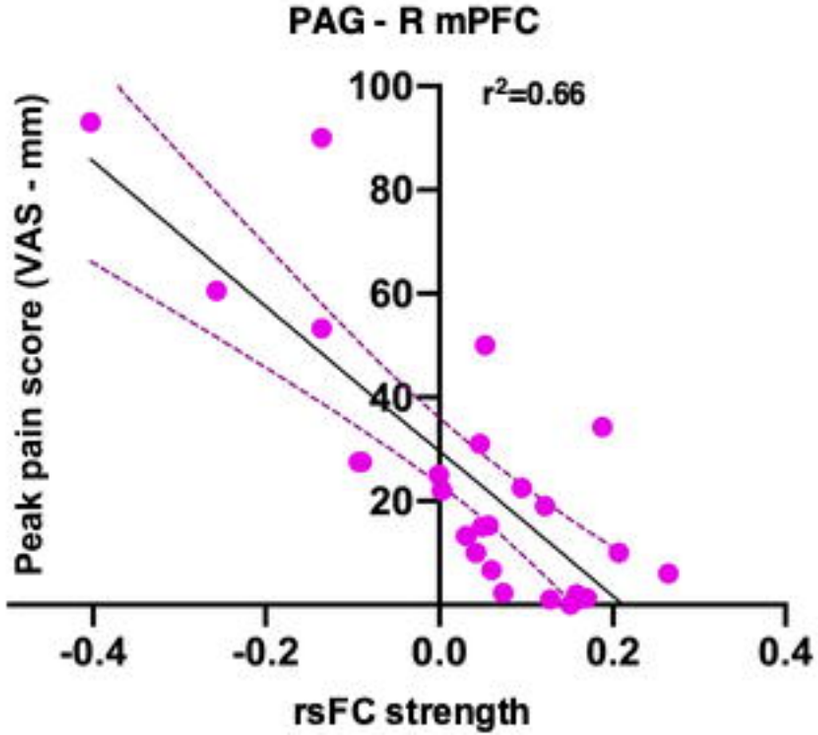
PAG - R mPFC
r²=0.66
Peak pain score (VAS - mm)
100
80
60
40
20
-0.4
-0.2
0.0
0.2
0.4
rsFC strength